The Impact of Model and Measurement Uncertainties on a State Estimation in Three-Phase Distribution Networks

Urban Kuhar, Miloš Pantoš, *Member, IEEE,* Gregor Kosec, and Aleš Švigelj, *Member, IEEE*

***Abstract*—In this paper we investigate the impact of model and measurement uncertainties on the state-estimation results for different estimators, and different measurement configurations in a three-phase distribution network. To obtain all the sensitivities of interest, the approach with a perturbation of the Karush-Kuhn-Tucker conditions was implemented. We express the sensitivities obtained in terms of uncertainty intervals rather than just partial derivatives. We also propose an upper error bound on the interval analysis. The presented approach has been used in a real-world scenario within the SUNSEED FP7 project to design the measurement configuration for a targeted state-estimation system's accuracy.**

I. Introduction

DISTRIBUTION networks are growing in complexity due to the increasing penetration of distributed generation and flexible demand. To ensure safe and stable operation in the future, the operators of distribution systems are adopting modern distribution-management systems (DMSs) that include tools for monitoring and controlling the network. Knowledge of the actual operating network state is obtained using the state-estimation (SE) algorithms that have been used in transmission networks for many years. However, there are some inherent differences that prevent their straightforward application in distribution networks. The most important issues are [1]:

- Load imbalance - distribution systems have many single-phase loads and therefore all three phases of the network need to be modeled.
- Low line X/R ratio - since the lines are smaller in diameter and shorter in length, their inductance is smaller, which in turn means that the phase displacement is smaller and harder to measure.
- Large number of nodes - this presents the need for a large number of measurements and increases the computational burden.
- Network model uncertainty - network parameters such as series impedances or shunt admittances (self and mutual) of the conductors might be incorrect as a result of inaccurate data provided by the manufacturer, inaccurate measurement campaigns, the effects of aging, etc. Measurement devices can become inaccurate due to ageing. All these errors impact the results of the SE.

In this paper we investigate the influence of uncertain model parameters and inaccurate (pseudo-) measurements on the estimated state variables in a three-phase distribution network for different measurement configurations and different estimators. The inputs, e.g., the line lengths, as well as the results, i.e., the state variables, are provided in terms of intervals rather than probability distribution functions. This is favorable from the engineering standpoint, since the intervals (e.g., $x \pm 10\%$) offer a more straightforward grasp of the possible range of variables than the variances do. The motivation for this work came from a real-world case, where the goal is to design a measurement configuration for a targeted state-estimation system's accuracy, which can be used in arbitrary, radial, multi-phase distribution networks.

Several methods were applied to the problem of sensitivity analyses in a power system's SE. In [2] the authors present a method that compares the covariance matrices of the true state vector based on the error-free model and a state vector that is based on a model with a known error. A comparison of the estimation bias and variance gives us a good measure for evaluating the modeling errors. The drawback of this method is that the complete calculation has to be repeated for every parameter that needs to be evaluated in terms of sensitivity. This quickly becomes unfeasible as the networks become larger than a few dozen buses. In [3], Macii et al. propose a similar technique that allows the computation of the uncertainty sensitivity coefficients for the complete measurement set. Their work, however, does not address the sensitivity calculation for model parameters and for quantities that are derived from the state variables, such as power flows or power injections. In [4] the authors propose a two-step method for the uncertainty analysis. First, the weighted least-squares (WLS) SE solution is computed and then the upper and lower interval bounds of the state variables are obtained using linear programming. If the inaccuracy in the measurements is modeled by the probability distribution function, then the calculated state vector is also modeled by the probability distribution function. Since the statistics of the measurement errors are difficult to characterize in practice, the idea here is that the accuracy of a particular measurement is described as, for example, $\pm 2\%$, rather than by the standard deviation or variance. The second step of the analysis allows the specifica-

U. Kuhar is with International Postgraduate School and the Department of Communication Systems, Jožef Stefan Institute, Ljubljana, Slovenia, e-mail: urban.kuhar@ijs.si

M. Pantoš is with the Laboratory of Power Systems, Faculty of Electrical Engineering, University of Ljubljana, Slovenia

G. Kosec and A. Švigelj are with the Department of Communication Systems, Jožef Stefan Institute, Ljubljana, Slovenia

tion of not just a single optimal estimate of the particular state variable, but also the uncertainty range within which we can be certain that the true value lies. The limitation of the method is that the lower and upper bounds need to be computed separately for each state variable, for each measurement. In [5] the authors expanded this approach to include the model parameters, as well. However, the limitation of the method to compute the lower and the upper bounds of the state variable for each variable separately, persists. In [6] a similar approach using the interval-analysis technique is proposed to find the bounds of the state variables for a power system whose line parameters lie within particular bounds. A linear measurement model is assumed, i.e., voltage phasor measurements only, other measurements are included by using the equivalent-measurements technique, i.e., measurements are converted into their equivalent voltage phasor values. In [7], [8], Chakrabarti et al. developed analytical expressions for the propagation of the uncertainty of the phasor measurement units (PMUs) in the SE algorithm. They also applied two other approaches, i.e., the Monte Carlo method and the random fuzzy variables. Line-parameter uncertainties are also not considered in their work. Reference [9] also describes the use of the Monte Carlo method for the evaluation of different uncertainty sources on a three-phase state estimator. In [10], Mínguez and Conejo leveraged a perturbation approach to sensitivity analysis based on the differentiation of the Karush-Kuhn-Tucker (KKT) conditions described in [11]. The distinctive advantage of the perturbation approach is that it yields all the sensitivities with respect to all the parameters at once and does not require multiple consecutive state estimation runs like the statistics based approaches. The method is thus suitable for evaluation of sensitivities of large networks. Another advantage of the perturbation approach is that it is agnostic to the choice of the estimator.

Our approach builds on [10], which we expanded with the following contributions: we expressed the uncertainties in terms of intervals and proposed an upper error bound on the interval analysis. We implemented several different estimators, namely the WLS estimator, the Least Absolute Value (LAV) [12] estimator, the Schweppe-Huber Generalized-M (SHGM) estimator based on projection statistics [13], and the Least Median of Squares (LMS) estimator [14], [15] and performed exhaustive comparisons of local sensitivities of those estimators. We give suggestions on the choice of the most suitable distribution system estimator for several different scenarios based on these comparisons. The analyses were performed for a full three-phase network model, which enables us to study how different uncertainties spread across phases.

This paper is organized as follows. Section II provides the three-phase state-estimation formulation. Section III provides a review of the sensitivity expressions derived by perturbation of the KKT conditions. In Section IV the results are presented for the IEEE distribution test feeder with 13 buses.

II. Three-Phase State Estimation

The state of a network can be deduced from various types of measurements, but in order to do that a relationship between the measurements and selected state variables must be established. This relationship is nonlinear, in general, and can be written as:

$$\mathbf{f} = \begin{bmatrix} f_1 \\ f_2 \\ \vdots \\ f_m \end{bmatrix} = \begin{bmatrix} h_1(x_1, \ldots, x_n) \\ h_2(x_1, \ldots, x_n) \\ \vdots \\ h_m(x_1, \ldots, x_n) \end{bmatrix} + \begin{bmatrix} w_1 \\ w_2 \\ \vdots \\ w_m \end{bmatrix} = \mathbf{h}(\mathbf{x}) + \mathbf{w} \tag{1}$$

where $\mathbf{f}$ is the vector of the measurements and $\mathbf{h}(\mathbf{x})$ is the vector of nonlinear functions relating the measurements to the vector of the state variables $\mathbf{x}$ that consists of voltage phasors in all the network buses. The symbol $\mathbf{w} \sim \mathcal{N}(\mathbf{0}, \mathbf{R})$ represents the noise contribution to the measurement vector. It is assumed that the noise in the measurements is uncorrelated and thus the measurement covariance matrix is $\mathbf{R} = diag\{\sigma_1^2, \sigma_2^2, \ldots, \sigma_m^2\}$.

A. State Estimators

Since the problem in Eqn. 1 is overdetermined ($m > n$), where m and n represent the number of measurements and the number of state variables, respectively, we define the weighted residual function for the i-th (i=1,...,m) measurement:

$$r_i = \frac{f_i - h_i(\mathbf{x})}{\sigma_i \gamma_i} \tag{2}$$

In general the estimation problem can be stated as the minimization of the following objective function:

$$J(\mathbf{x}, \mathbf{a}) = \sum_{i=1}^{m} \gamma_i^2 \rho(r_i) \tag{3}$$

The estimators then differ by the choice of the ρ function and the γ weight.

1) Weighted Least Squares estimator: The WLS estimator is a quadratic form of the maximum likelihood estimator. It can be stated as the minimisation of the following objective function:

$$J(\mathbf{x}, \mathbf{a}) = \sum_{i=1}^{m} r_i^2 \tag{4}$$

where $\rho(r_i) = 1/2 \cdot r_i^2$ and $\gamma_i = 1$. An estimate of the state can be obtained iteratively using the Gauss-Newton method, see [16] for example.

2) Least Absolute Value estimator: LAV estimator is based on the minimization of the $\mathcal{L}_1$ norm of weighted measurement residual [17]. It can be stated as the minimisation of the following objective function:

$$J(\mathbf{x}, \mathbf{a}) = \sum_{i=1}^{m} |r_i| \tag{5}$$

where $\rho(r_i) = |r_i|$ and $\gamma_i = 1$. This is essentially a linear programming problem that can be solved with any of the existing techniques such as primal dual interior point method [18], iteratively re-weighted least squares [12], or a simplex based algorithm [16].

3) SHGM estimator based on projection statistics: This method implements a projection algorithm that accounts for the sparsity of the Jacobian matrix. It assigns to each data point a projection statistics. Based on these projection statistics, a robustly weighted estimator is defined [13] as:

$$\rho(r_i) = \begin{cases} \frac{1}{2}r_i^2 & |r_i| \leq c \\ c|r_i| - \frac{c^2}{2} & otherwise \end{cases} \tag{6}$$

where:

$$\gamma_i = \min\Big\{1, \Big(\frac{b_i}{PS_i}\Big)^2\Big\}, \tag{7}$$

$$b_i = \chi^2_{\xi,0.975}, \tag{8}$$

$$PS_i = \max_{\mathbf{H}_k} \frac{|\mathbf{H}_i \mathbf{H}_k^T|}{\beta_i} \;\; k = 1, 2, \ldots, m, \tag{9}$$

$$\beta_i = 1.1926 \cdot \text{lomed}_i\Big\{\text{lomed}_{i \neq j}|\mathbf{H}_i\mathbf{H}_k^T + \mathbf{H}_j\mathbf{H}_k^T|\Big\}, \tag{10}$$

$\mathbf{H}_i$ is the i-th row vector of the Jacobian matrix $\mathbf{H}$, ξ is the number of nonzero entries in the corresponding (i-th) row of the Jacobian matrix, and a good choice for c ranges from 1 to 3 (selected in our case). For more detailed explanation of the estimator please see [13].

The presented estimation problem can be solved using the iteratively reweighted least squares (IRLS) algorithm.

4) Least Median of Squares estimator: The LMS estimator is a high breakdown point estimator that minimizes the ν-th ordered squared residual, yielding:

$$J(\mathbf{x}, \mathbf{a}) = r_\nu^2, \tag{11}$$

where:

$$\nu = \frac{m}{2} + \frac{n+1}{2}. \tag{12}$$

Residuals are first squared and then ordered by increasing value: $r_1^2 \leq \ldots \leq r_m^2$. r_ν^2 is the ν-th largest of these quantities.

The computation of the LMS estimates requires the combinatorial procedure which repeatedly selects set of measurements of size n for which the system is observable. For each selected set of measurements, the nonlinear system is solved by the Gauss-Newton method, the weighted residuals determined, and ordered by increasing squared values. The LMS estimates are then found by minimizing the objective function among the selected measurement sets. Since the full combinatorial search becomes computationaly infeasible even for small systems, different approaches are used to reduce the number of combinations in the search space, see [14], [15].

B. Three-Phase Branch Model

Functions that relate measurements to the vector of state variables are developed from a three-phase branch model [19] in Fig. 1. The node voltage phasors are denoted as: $E_m^a = |V_m^a|e^{j\phi_m^a}$, where $|V_m^a|$ represents the phasor magnitude, and ϕ_m^a represents a phase angle at the node m on phase a. The self and mutual series impedances are denoted as z_{km}^{xy}, where k and m are buses and x and y are phases on the buses k and m, respectively. $\mathbf{Y}_{km,sh}$ is the matrix of self and mutual shunt admittances. The matrices $\mathbf{T}_{km}$ and $\mathbf{T}_{mk}$ are used for the modeling of voltage regulators and tap changers.

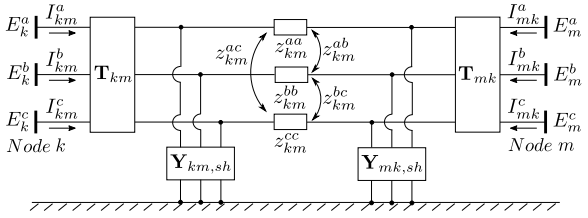

Fig. 1. Three-phase unified branch model

Formulation of the state-estimation problem usually includes active and reactive line power flow and active and reactive node power-injection measurements, as well. Expressions for them are provided in Eqn. 16, Eqn. 17, Eqn. 18, and Eqn. 19 respectively, where $y_{km}^{aa} = g_{km}^{aa} + jb_{km}^{aa}$ is the branch series admittance, and G_{km}^{ap} and B_{km}^{ap}, respectively, represent the real and imaginary components of the (a, p) element of the (k, m) system-admittance submatrix, and κ is the set of buses adjacent to bus k, including bus k. Ω_p denotes the set of phases $\{a, b, c\}$.

Considering the cost function, the state-estimation problem can be formulated as an optimization problem including constraints:

$$\begin{aligned} \underset{\mathbf{x}}{\text{minimize}} \quad & J(\mathbf{x}, \mathbf{a}) \\ \text{subject to} \quad & \mathbf{c}(\mathbf{x}, \mathbf{a}) = 0 : \boldsymbol{\lambda}, \\ & \mathbf{g}(\mathbf{x}, \mathbf{a}) \leq 0 : \boldsymbol{\mu}, \end{aligned} \tag{13}$$

where $\mathbf{x} \in \mathbb{R}^n$, $\mathbf{a} \in \mathbb{R}^p$, $J(\mathbf{x}, \mathbf{a})$ is a scalar cost function, $\mathbf{c}(\mathbf{x}, \mathbf{a})$ is the vector of equality constraints representing exactly known pseudo-measurements (zero injections), $\mathbf{g}(\mathbf{x}, \mathbf{a})$ is the vector of inequality constraints (e.g., the phase angles must be smaller than $\frac{\pi}{2}$), and $\boldsymbol{\lambda}$ and $\boldsymbol{\mu}$ are the Lagrange multiplier vectors for the equality and inequality constraints, respectively. Note that vector $\mathbf{a}$ includes measurements and model data that are of interest in the calculation of sensitivities. In our case it includes all the measurements and all the system-admittance elements, i.e., $\mathbf{G}$, $\mathbf{B}$, $\mathbf{b}_{shunt}$, and $\mathbf{g}_{shunt}$.

III. Perturbation Approach to Sensitivity Analysis

A. Sensitivities

We are interested in the sensitivities around the current operating point, thus the first step towards obtaining sensitivities is to calculate the optimal solution for the current state-estimation problem, i.e., the problem in Eqn. 13 needs to be solved. The solution is denoted as ($\mathbf{x}^*$, $\mathbf{a}$, $\boldsymbol{\lambda}^*$). Note that inactive, i.e., non-binding, inequality constraints are disregarded, and the active ones are incorporated as equality constraints. Then the KKT conditions are stated for the optimal solution:

$$\nabla_{\mathbf{x}} J(\mathbf{x}^*, \mathbf{a}) + \sum_{k=1}^{l} \lambda_k^* \nabla_{\mathbf{x}} c_k(\mathbf{x}^*, \mathbf{a}) = \mathbf{0} \tag{14}$$

$$c_k(\mathbf{x}^*, \mathbf{a}) = 0, k = 1, 2, \ldots, l, \tag{15}$$

where $\nabla_{\mathbf{x}}$ represents the gradient with respect to vector $\mathbf{x}$, and l is the total number of equality and active inequality constraints. As the sensitivity analysis needs information about

$$P^a_{km} = |V^a_k| \sum_{j\in\Omega_p}\sum_{n\in\Omega_p}\sum_{i\in\Omega_p} \Big\{ t^{ni}_{km} t^{aj}_{km} |V^i_k| \Big[(g^{jn}_{km} + g^{jn}_{km,sh}) cos(\phi^a_k - \phi^i_k) + (b^{jn}_{km} + b^{jn}_{km,sh}) sin(\phi^a_k - \phi^i_k) \Big] - t^{ni}_{mk} t^{aj}_{km} |V^i_m| \Big[g^{jn}_{km} cos(\phi^a_k - \phi^i_m) + b^{jn}_{km} sin(\phi^a_k - \phi^i_m) \Big] \Big\} \tag{16}$$

$$Q^a_{km} = |V^a_k| \sum_{j\in\Omega_p}\sum_{n\in\Omega_p}\sum_{i\in\Omega_p} \Big\{ t^{ni}_{km} t^{aj}_{km} |V^i_k| \Big[(g^{jn}_{km} + g^{jn}_{km,sh}) sin(\phi^a_k - \phi^i_k) - (b^{jn}_{km} + b^{jn}_{km,sh}) cos(\phi^a_k - \phi^i_k) \Big] - t^{ni}_{mk} t^{aj}_{km} |V^i_m| \Big[g^{jn}_{km} sin(\phi^a_k - \phi^i_m) - b^{jn}_{km} cos(\phi^a_k - \phi^i_m) \Big] \Big\} \tag{17}$$

$$P^a_k = |V^a_k| \sum_{m\in\kappa}\sum_{p\in\Omega_p} |V^p_m| \big(G^{ap}_{km} cos(\phi^a_k - \phi^p_m) + B^{ap}_{km} sin(\phi^a_k - \phi^p_m) \big) \tag{18}$$

$$Q^a_k = |V^a_k| \sum_{m\in\kappa}\sum_{p\in\Omega_p} |V^p_m| \big(G^{ap}_{km} sin(\phi^a_k - \phi^p_m) - B^{ap}_{km} cos(\phi^a_k - \phi^p_m) \big) \tag{19}$$

the dual problem, the required step before the sensitivity study is to obtain the dual variables solving the linear system of equations that is obtained from Eqn. 14. In the next step the KKT conditions are perturbed. The perturbation must be made in such way that the KKT conditions still hold [11]. The system of equations is then formed as follows:

$$\begin{bmatrix} \mathbf{F_{xx}} & \mathbf{F_{xa}} & \mathbf{C_x}^T \\ \mathbf{C_x} & \mathbf{C_a} & \mathbf{0} \end{bmatrix} \cdot \begin{bmatrix} d\mathbf{x} \\ d\mathbf{a} \\ d\boldsymbol{\lambda} \end{bmatrix} = \mathbf{0} \tag{20}$$

where the vectors and submatrices (including their dimensions) are:

$$\mathbf{F}_{\mathbf{xx}(n\times b)} = \nabla_{\mathbf{xx}} J(\mathbf{x}^*, \mathbf{a}) + \sum_{k=1}^{l} \lambda^*_k \nabla_{\mathbf{xx}} c_k(\mathbf{x}^*, \mathbf{a}), \tag{21}$$

$$\mathbf{F}_{\mathbf{xa}(n\times p)} = \nabla_{\mathbf{xa}} J(\mathbf{x}^*, \mathbf{a}) + \sum_{k=1}^{l} \lambda^*_k \nabla_{\mathbf{xa}} c_k(\mathbf{x}^*, \mathbf{a}), \tag{22}$$

$$\mathbf{C}_{\mathbf{x}(l\times n)} = \big[\nabla_{\mathbf{x}} \mathbf{c}(\mathbf{x}^*, \mathbf{a}) \big]^T, \tag{23}$$

$$\mathbf{C}_{\mathbf{a}(l\times p)} = \big[\nabla_{\mathbf{a}} \mathbf{c}(\mathbf{x}^*, \mathbf{a}) \big]^T, \tag{24}$$

where $\nabla_{\mathbf{a}}$ represents the gradient with respect to vector $\mathbf{a}$, $\nabla_{\mathbf{xx}}$ and $\nabla_{\mathbf{xa}}$ represent the Hessian with respect to vectors $\mathbf{x}$ and $\mathbf{x}$, $\mathbf{a}$, respectively, and p is the dimension of vector $\mathbf{a}$.

To calculate the sensitivities of the state vector with respect to the data vector, the system in Eqn. 16 is reformulated as:

$$\mathbf{U} \begin{bmatrix} d\mathbf{x} & d\boldsymbol{\lambda} \end{bmatrix}^T = \mathbf{S} d\mathbf{a} \tag{25}$$

where the matrices $\mathbf{U}$ and $\mathbf{S}$ are:

$$\begin{aligned} \mathbf{U} &= \begin{bmatrix} \mathbf{F_{xx}} & \mathbf{C_x^T C_x} & \mathbf{0} \end{bmatrix} \\ \mathbf{S}^T &= - \begin{bmatrix} \mathbf{F_{xa}} & \mathbf{C_a} \end{bmatrix} \end{aligned} \tag{26}$$

from which it follows that:

$$\begin{bmatrix} \frac{\partial \mathbf{x}}{\partial \mathbf{a}} & \frac{\partial \boldsymbol{\lambda}}{\partial \mathbf{a}} \end{bmatrix}^T = \mathbf{U}^{-1} \mathbf{S}. \tag{27}$$

The solution to the system in Eqn. 27 yields sensitivity expressions with respect to the data vector $\mathbf{a}$, which contains the measurements and system-admittance elements. From an engineering perspective important parameters are the sensitivities with respect to the conductor lengths, i.e., their impedances (since the conductor resistances and reactances are linearly dependent on the conductor's length [20]). The chain rule must be used to obtain the sensitivities with respect to the line impedances from sensitivities with respect to the admittance elements.

Besides the sensitivities of the state variables, the sensitivities of the derived variables, such as power flows or power injections, are also of interest. The way to obtain them is again with the application of the chain rule.

The LAV, LMS, and SHGM estimators produce objective functions that have discontinuous derivatives. Since we are interested in small deviations of model and measurement parameters, we do not operate in the area of discontinuities with the SHGM and LMS estimators. This is not the case for the LAV estimator where discontinuity is encountered at $r_i = 0$. For the LAV estimator the problem is restated as:

$$J(\mathbf{x}, \mathbf{a}) = \sum_{i=1}^{m} r_i \tag{28}$$

and the measurements are imposed as constraints [21], i.e. $\big(f_i - h_i(\mathbf{x})\big)/\sigma_i \leq r_i$ and $\big(f_i - h_i(\mathbf{x})\big)/\sigma_i \geq -r_i$.

B. Implementation validation

The perturbation approach to implementation of the sensitivity analysis was validated by comparing the obtained results with direct numerical derivatives. The measurements were generated from the load-flow results for the reference feeder loading provided by the IEEE [22], more precisely the validation was performed on the 13-bus IEEE distribution test feeder [22] shown in Fig. 2 (labels on the branches represent the phasing sequence, labels near the spot loads represent the load type and its connection (D - delta connection, Y - wye connection, PQ - constant power injection load, Z - constant impedance load, I - constant current load)). The validation was made on a single configuration of measurements, which is listed in Table I. The PMU column indicates the presence of

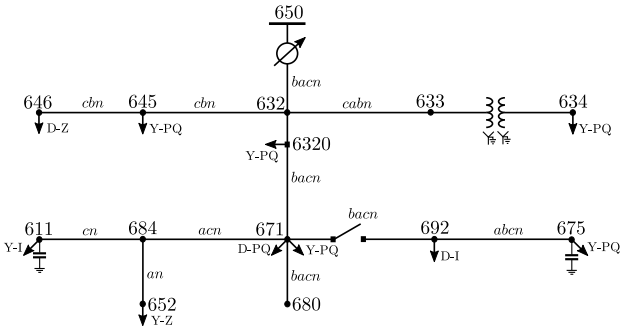

Fig. 2. The 13-bus IEEE test feeder

TABLE I
MEASUREMENT CONFIGURATION FOR VALIDATION

Bus ID	PMU	PQ injection	Equality constr.
650			
632	•		•
633	•		•
634		•	
645	•		
646		•	
6320	•		
671	•		
692	•		
675		•	
680		•	•
684	•		•
652		•	
611		•	

a PMU measurement on a corresponding bus, the PQ injection bus indicates the presence of an active/reactive power-injection measurement on the corresponding bus, and the equality constr. column indicates whether zero injection constraints are imposed on the corresponding bus. For validation purposes the measurements were assumed to be perfectly accurate without added noise. The direct numerical derivatives were computed as follows: first, the state estimation was computed to obtain the reference state vector $\mathbf{x}_{ref}$, then the parameter in question was perturbed $a + \Delta a$ and the state estimation was computed again with a perturbation, to obtain the state vector $\mathbf{x}_p$ the derivatives were then obtained as follows:

$$\frac{\partial \mathbf{x}}{\partial a} \approx \frac{\mathbf{x}_p - \mathbf{x}_{ref}}{\Delta a}. \tag{29}$$

The case presented here is the phase-angle sensitivity across all buses with respect to the active power measurement on bus 634. The results are shown in Fig. 3. Similar results were obtained for other cases.

Note that each calculation of the direct numerical derivative requires the computation of the complete SE problem, which is computationally intensive. The direct approach thus becomes infeasible for networks larger than several dozen buses. However, the implementation of the direct numerical derivation is much simpler and thus less prone to error and we selected this approach to verify the implementation of the perturbation approach. The upper graph in the subplot (Fig. 3) shows the results obtained with the perturbation of the KKT conditions. The lower graph represents the error with respect

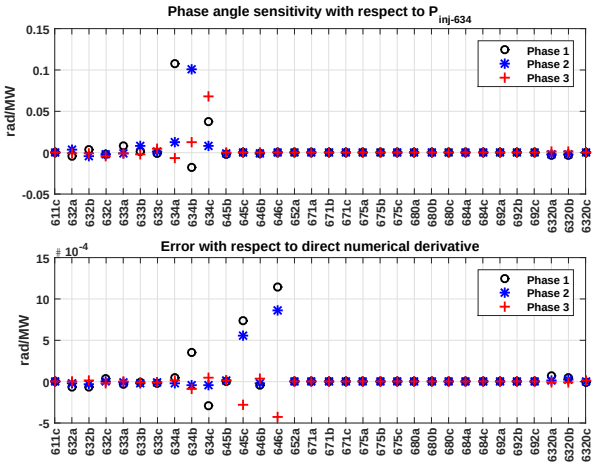

Fig. 3. Sensitivity of phase angles with respect to the active power measurement on bus 634

to the direct numerical derivative. It is clear that there is some difference between the perturbation approach results and the direct numerical derivatives. This difference is attributed to numerical errors, since in the perturbation approach all the derivatives are also computed numerically.

C. Error Bound

The sensitivities obtained with the solution to the system in Eqn. 27 represent tangent lines at the optimal solution point. These derivatives are only truly valid for that point; however, from an engineering perspective we are more interested in intervals, e.g., we would like to know within which interval we can expect the state vector to be if we are confident that the line length is within a certain range.

The interval $[-\mathbf{x}_a, \mathbf{x}_a]$ can be obtained from:

$$\pm\mathbf{x}_a \approx \mathbf{x}^* \pm \Delta\mathbf{x} = \mathbf{x}^* \pm \Delta a \frac{\partial \mathbf{x}}{\partial a}. \tag{30}$$

Since the derivative is only valid for the optimal solution, an error will invariably be made with such an interval calculation.

An example for the phase part of the state-vector error is shown in Fig. 4, for $684 - 652$ conductor impedance ($z_{684a-652a}$). The error is computed as:

$$E = max\left|\mathbf{x}_{true} - (\mathbf{x}^* + \Delta z_{684a-652a} \frac{\partial \mathbf{x}^*}{\partial z_{684a-652a}})\right| \tag{31}$$

The conductor has a specified length of 800 feet, while the computation was performed for an impedance interval corresponding to a conductor length in the range from 600 to 1000 feet ($\pm 25\%$). It is clear that though the error is small it quickly increases as we move away from the value at the optimal solution $\mathbf{x}^*$. Thus, a bound that would specify the maximum state vector error when a parameter interval analysis is performed is of interest. The error bound for the linear approximation would normally require knowledge of the second-order derivatives $\frac{\partial^2 \mathbf{x}}{\partial \mathbf{a}^2}$. Calculating them is impracticable for the problem at hand.

Another approach is to take advantage of the nature of the problem and the radial topology of the distribution systems.

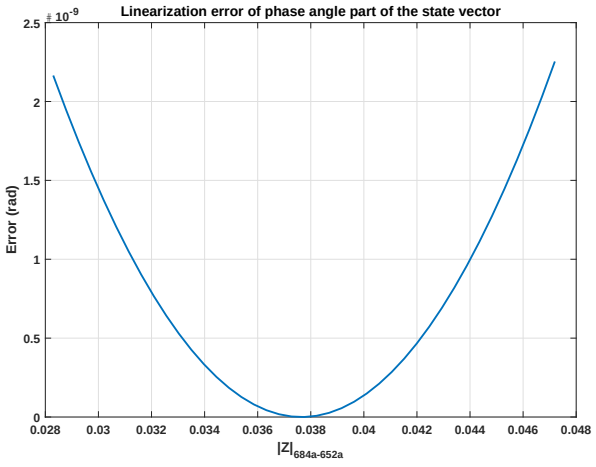

Fig. 4. Linearization error of phase-angle part of the state vector

The only two things that influence the state variables are the line impedances and the feeder loading. In radial networks the largest decrease of the state variables (voltage magnitudes and phase angles) is achieved when the estimated feeder loading is the largest and when the given line impedances are the greatest (and vice versa). We have performed simulations that illustrate this fact. Simulations were performed for six different feeder loadings and line impedances. For each run the loads as well as line impedances were increased. Figs. 5 and 6 depict that voltage magnitudes and voltage phases decrease on all the buses for each consecutive run. From this the rules for data

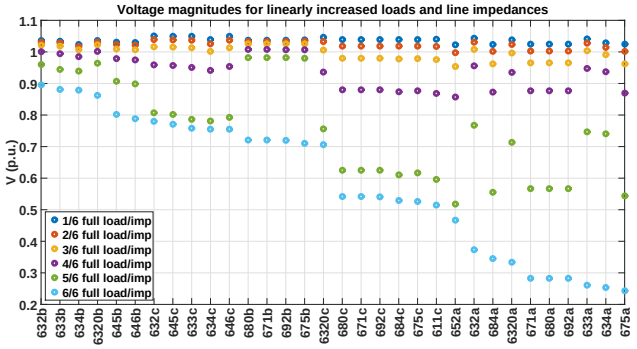

Fig. 5. Voltage magnitudes for linearly increased loads and impedances

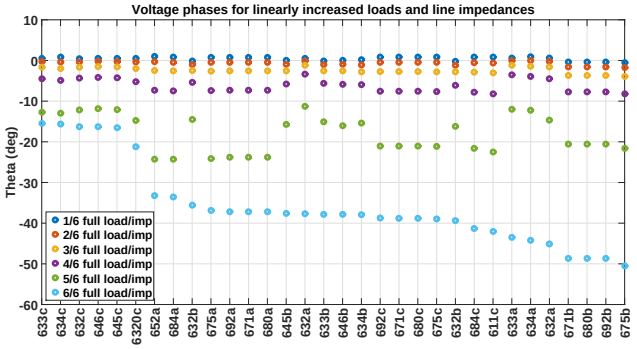

Fig. 6. Voltage phases for linearly increased loads and impedances

vectors $\mathbf{a}_u$ and $\mathbf{a}_l$ that will yield the state vectors with the largest deviation from $\mathbf{x}^*$ in both directions (i.e., $\mathbf{x}_u$ and $\mathbf{x}_l$) can be inferred. For power-injection and flow measurements the upper and lower interval bounds are taken for $\mathbf{a}_u$ and $\mathbf{a}_l$, respectively:

$$\{\mathbf{P}_{i,u}, \mathbf{Q}_{i,u}, \mathbf{P}_{ij,u}, \mathbf{Q}_{ij,u}\} = \{\mathbf{P}_i, \mathbf{Q}_i, \mathbf{P}_{ij}, \mathbf{Q}_{ij}\} + \{\mathbf{\Delta P}_i, \mathbf{\Delta Q}_i, \mathbf{\Delta P}_{ij}, \mathbf{\Delta Q}_{ij}\} \quad (32)$$

$$\{\mathbf{P}_{i,l}, \mathbf{Q}_{i,l}, \mathbf{P}_{ij,l}, \mathbf{Q}_{ij,l}\} = \{\mathbf{P}_i, \mathbf{Q}_i, \mathbf{P}_{ij}, \mathbf{Q}_{ij}\} - \{\mathbf{\Delta P}_i, \mathbf{\Delta Q}_i, \mathbf{\Delta P}_{ij}, \mathbf{\Delta Q}_{ij}\} \quad (33)$$

For line resistances and reactances the upper interval bounds are also used:

$$\{\mathbf{r}_{ij,u}, \mathbf{x}_{ij,u}\} = \{\mathbf{r}_{ij}, \mathbf{x}_{ij}\} + \{\mathbf{\Delta x}_{ij}, \mathbf{\Delta r}_{ij}\} \quad (34)$$

$$\{\mathbf{r}_{ij,l}, \mathbf{x}_{ij,l}\} = \{\mathbf{r}_{ij}, \mathbf{x}_{ij}\} - \{\mathbf{\Delta x}_{ij}, \mathbf{\Delta r}_{ij}\} \quad (35)$$

For voltage magnitudes the lower interval bounds are used:

$$|\mathbf{V}|_{i,u} = |\mathbf{V}|_i - \mathbf{\Delta}|\mathbf{V}|_i \quad (36)$$

$$|\mathbf{V}|_{i,l} = |\mathbf{V}|_i + \mathbf{\Delta}|\mathbf{V}|_i \quad (37)$$

For the voltage phase angles the lower interval bounds are also used:

$$\mathbf{\Theta}_{i,u} = \mathbf{\Theta}_i - \mathbf{\Delta\Theta}_i \quad (38)$$

$$\mathbf{\Theta}_{i,l} = \mathbf{\Theta}_i + \mathbf{\Delta\Theta}_i \quad (39)$$

The data vectors are thus formed as:

$$\mathbf{a}_u = \big[\mathbf{P}_{i,u}, \mathbf{Q}_{i,u}, \mathbf{P}_{ij,u}, \mathbf{Q}_{ij,u}, \mathbf{r}_{ij,u}, \mathbf{x}_{ij,u}, |\mathbf{V}|_{i,u}, \mathbf{\Theta}_{i,u}\big]. \quad (40)$$

$$\mathbf{a}_l = \big[\mathbf{P}_{i,l}, \mathbf{Q}_{i,l}, \mathbf{P}_{ij,l}, \mathbf{Q}_{ij,l}, \mathbf{r}_{ij,l}, \mathbf{x}_{ij,l}, |\mathbf{V}|_{i,l}, \mathbf{\Theta}_{i,l}\big]. \quad (41)$$

Using them, the state vectors $\mathbf{x}_u$ and $\mathbf{x}_l$ are obtained. With the obtained state vectors, the upper error bounds on the interval calculations can be specified as:

$$\left|\mathbf{x}_u - \left(\mathbf{x}^* + \Delta a \frac{\partial \mathbf{x}^*}{\partial a}\right)\right| \geqslant \left|\mathbf{x}_{true} - \left(\mathbf{x}^* + \Delta a \frac{\partial \mathbf{x}^*}{\partial a}\right)\right| \quad \forall a \in [\mathbf{a}, \mathbf{a}_u] \quad (42)$$

$$\left|\mathbf{x}_l - \left(\mathbf{x}^* + \Delta a \frac{\partial \mathbf{x}^*}{\partial a}\right)\right| \geqslant \left|\mathbf{x}_{true} - \left(\mathbf{x}^* + \Delta a \frac{\partial \mathbf{x}^*}{\partial a}\right)\right| \quad \forall a \in [\mathbf{a}, \mathbf{a}_l] \quad (43)$$

These error bounds only apply to radial networks.

IV. Results

The sensitivity calculations were performed for the three different measurement configurations that are listed in Table II, and for four different estimators, namely WLS, LAV, SHGM, and LMS. For each configuration the sensitivities of the state variables with respect to the measurements and the conductor impedances (self and mutual) were of interest. Different measurement configurations and estimators yield a large number of possible combinations, and although we conducted an exhaustive number of simulations, we choose to depict the most interesting results. The following subsections provide results for the uncertain conductor length, and the uncertain measurements.

TABLE II
MEASUREMENT CONFIGURATION FOR VALIDATION

Configuration	PQ		PQ-PMU		PMU-PQ	
Bus ID	PQ	PMU	PQ	PMU	PQ	PMU
632	•		•	•	•	•
633	•		•	•	•	•
634	•		•	•		•
645	•		•	•	•	•
646	•		•	•		•
6320	•		•	•		•
671	•		•	•		•
692	•		•	•		•
675	•		•	•	•	•
680	•		•	•	•	•
684	•		•	•		•
652	•		•	•	•	•
611	•		•	•	•	•

A. *Variation of the line length*

The line between buses 6320 and 671 is 1500 feet long. A $\pm 20\%$ interval accounts for ± 300 feet. Since the line has a three-phase configuration the line impedance matrix has three self-impedances and three mutual-impedances.

1) Measurement configuration PQ: Figs. 7 and 8 show the interval of the magnitude and phase parts of the state vector respectively, with respect to the $z_{6320-671}$ for the SHGM and WLS estimators. It is clear that the local sensitivity of the two estimators is almost identical.

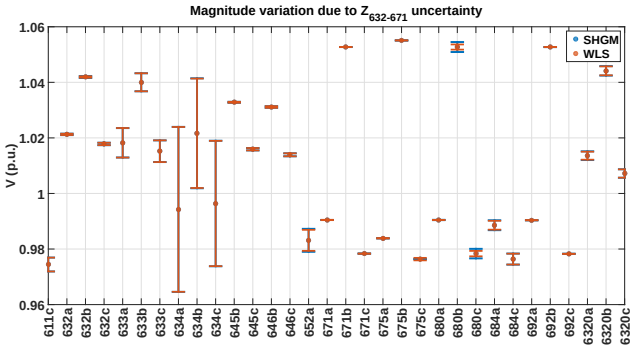

Fig. 7. Interval of the magnitude part of the state vector due to uncertain $\mathbf{Z}_{6320-671}$

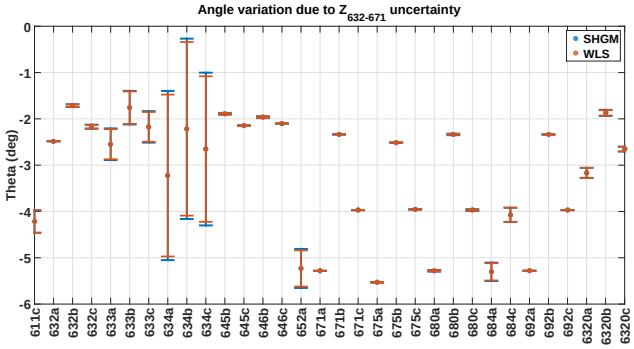

Fig. 8. Interval of the angle part of the state vector due to uncertain $\mathbf{Z}_{6320-671}$

Figs. 9 and 10 show the local sensitivity for the LAV estimator with comparison to WLS. It is clear that the influence of uncertain line length is much smaller when the LAV estimator is used. Further, the uncertainty interval is the largest on

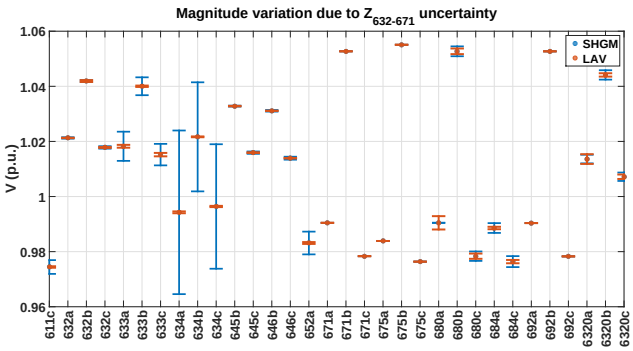

Fig. 9. Interval of the magnitude part of the state vector due to uncertain $\mathbf{Z}_{6320-671}$

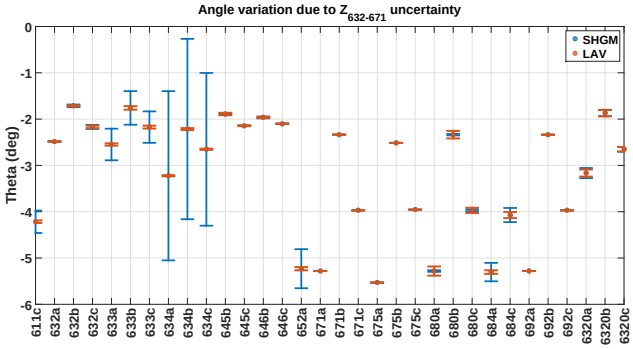

Fig. 10. Interval of the angle part of the state vector due to uncertain $\mathbf{Z}_{6320-671}$

buses 633 and 634, the probable reason for this is that the series impedance of the transformer on branch $633-634$ is two orders of magnitude higher than the series impedance of any other branch. The uncertainty spreads across all the buses due to the measurement configuration and the nature of power injection measurement functions (Eqn. 18 and Eqn. 19).

Note that LMS estimator was not added to the comparisons because there are no redundant measurements, i.e. if we construct a subset from the existing measurements the system becomes unobservable.

2) Measurement configuration PQ-PMU: In this measurement configuration the effect on the estimated state variables is much smaller for the WLS and SHGM estimators and remains negligible for the LAV estimator as Figs. 11 and 12 show. The results for the LMS estimator are almost identical to SHGM estimator.

3) Measurement configuration PMU-PQ: The effect of the uncertain line length on the state vector in this configuration is even smaller than that in the previous two configurations, for all four estimators. Figs. 13 and 14 depict results for WLS and LMS estimators. The two are virtually indistinguishable. We omitted the results for SHGM and LAV, but the results are no different for these two estimators.

The reason for such small influence can be found in the measurement configuration in which PMUs represent the majority of devices. Phase-angle and magnitude measurements

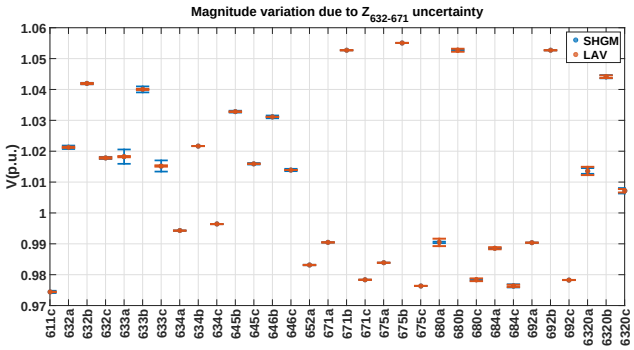

Fig. 11. Interval of the magnitude part of the state vector due to uncertain $\mathbf{Z}_{6320-671}$

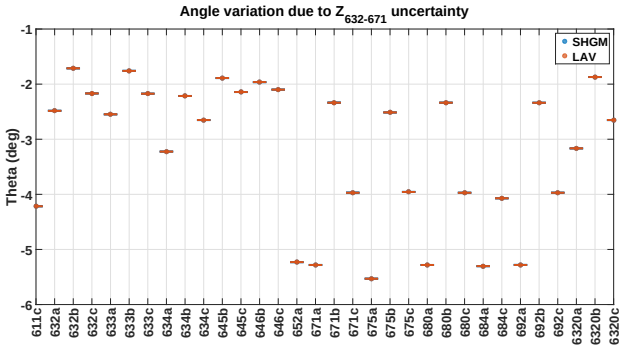

Fig. 12. Interval of the angle part of the state vector due to uncertain $\mathbf{Z}_{6320-671}$

alone form a linear state-estimation problem, where topology has no effect on the state variables. With the introduction of additional power-injection measurements the topology has an effect on certain state variables, but since the measurements are only placed on a few buses and the influence of topology uncertainty spreads in accordance with Eqn. 18 and Eqn. 19 some buses remain isolated from the uncertainty influence.

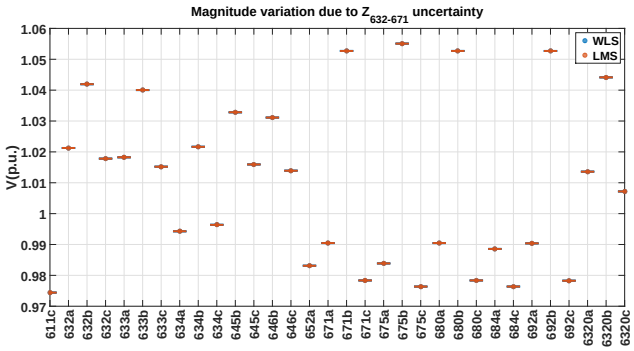

Fig. 13. Interval of the magnitude part of the state vector due to uncertain $\mathbf{Z}_{6320-671}$

B. Quality of measurements

For each of the measurement configurations and different estimators the effect of uncertain measurements was computed. Different measurement weights determine the magnitude of the influence of a particular measurement in comparison to

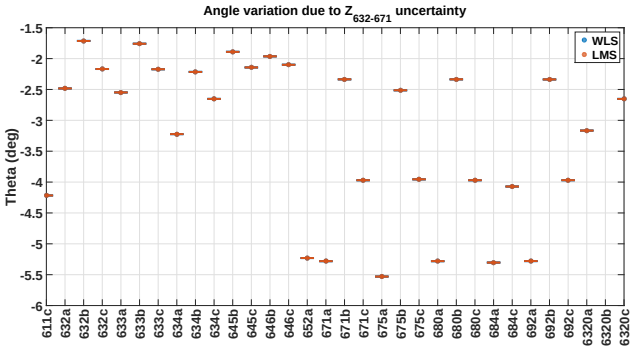

Fig. 14. Interval of the angle part of the state vector due to uncertain $\mathbf{Z}_{6320-671}$

the others, but to simplify the problem, here all measurements have the same weights.

1) Measurement configuration PQ: The variation of the state vector for a $\pm 20\%$ uncertainty interval on power-injection measurements on bus 671 is shown in Fig. 15 and Fig. 16 for the estimators WLS and SHGM. It is clear that the estimators have a similar local sensitivity. Surprisingly the LAV estimator has a much greater local sensitivity as is depicted in Figs. 17 and 18.

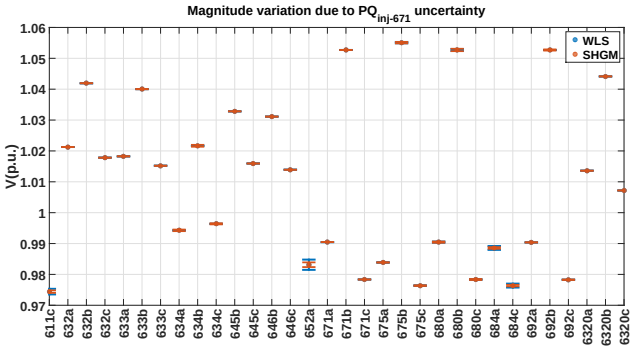

Fig. 15. Interval of the magnitude part of the state vector due to uncertain $\mathbf{PQ}_{inj-671}$

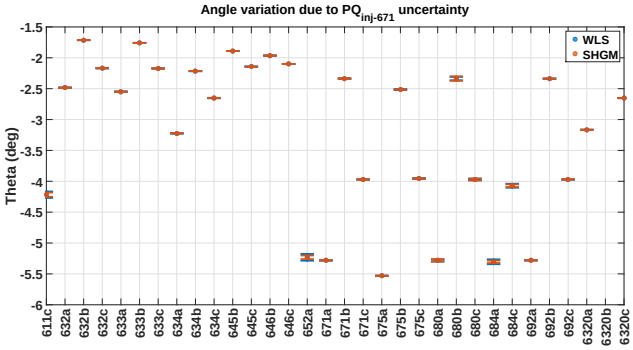

Fig. 16. Interval of the angle part of the state vector due to uncertain $\mathbf{PQ}_{inj-671}$

2) Measurement configuration PQ-PMU: The variation of the state vector for a $\pm 20\%$ uncertainty interval of the power injection measurement on bus 671 is shown in Figs. 19 20. It is

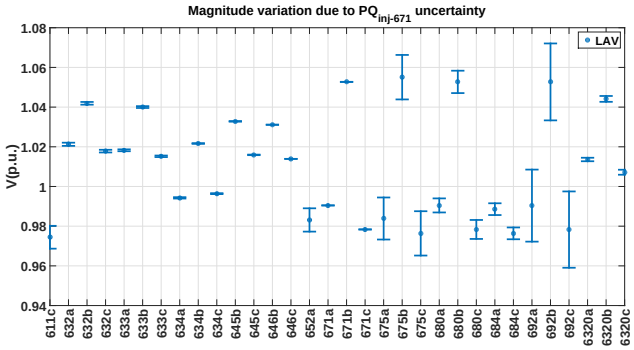

Fig. 17. Interval of the magnitude part of the state vector due to uncertain $\mathbf{PQ}_{inj-671}$

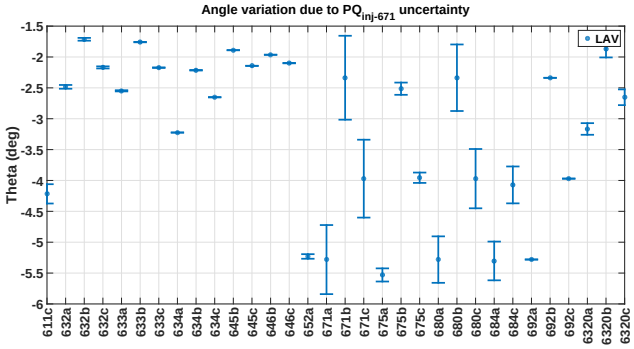

Fig. 18. Interval of the angle part of the state vector due to uncertain $\mathbf{PQ}_{inj-671}$

clear that the angle-measurement variation is barely observable in both the LAV and SHGM estimators. Interestingly, it can be observed that, similarly to the PQ configuration, the LAV estimator has larger local sensitivity on the magnitude part than the SHGM. The WLS and LMS estimators behave much like the SHGM.

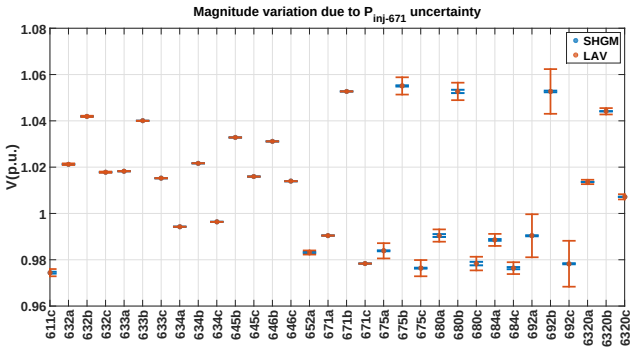

Fig. 19. Interval of the magnitude part of the state vector due to uncertain $\mathbf{PQ}_{inj-671}$

3) Measurement configuration PMU-PQ: Fig. 21 and Fig. 22 show the state vector uncertainty interval for $\pm 0.01 p.u.$ uncertain phase measurements on bus 634. It is clear that the angle-measurement variation is almost fully translated into the state vector on buses 634 and 633, but remains isolated on the phase part of these two buses. Again, the reasons for this are to be found in the measurement configuration. The

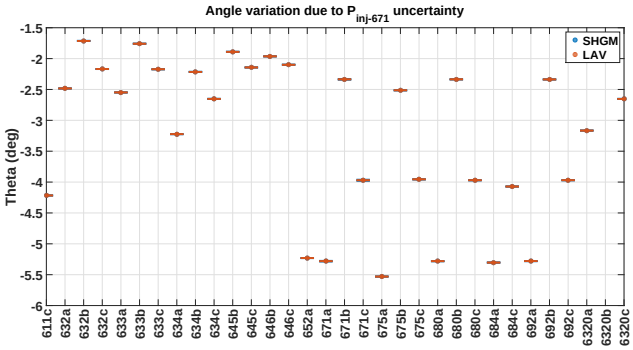

Fig. 20. Interval of the angle part of the state vector due to uncertain $\mathbf{PQ}_{inj-671}$

power injection measurement on bus 634 causes a spread of the uncertainty onto the adjacent bus.

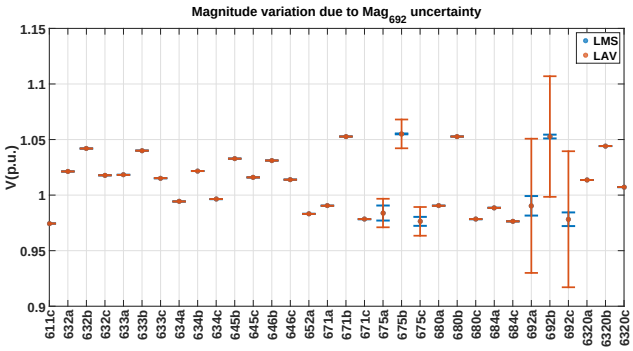

Fig. 21. Interval of the magnitude part of the state vector due to uncertain $|\mathbf{V}|_{692}$

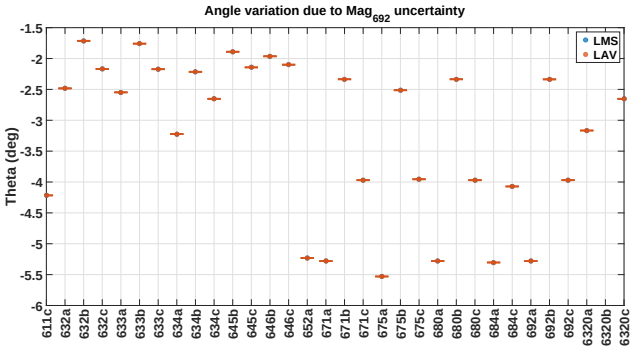

Fig. 22. Interval of the angle part of the state vector due to uncertain $|\mathbf{V}|_{692}$

V. Conclusion

In this paper we investigated the local sensitivities of estimated state variables with respect to the uncertain line lengths and inaccurate (pseudo-) measurements in a three-phase distribution network for different measurement configurations and different estimators. We selected and implemented the approach with a perturbation of the KKT conditions, which is agnostic to the choice of the estimator. The analysis was performed for a full three-phase branch network model. The implemented estimators were LAV, WLS, LMS and SHGM.

The results show that both the measurement configuration and the estimator choice have a large influence on the spread of the line-impedance and measurement uncertainties across the network buses in the estimated state vector. The LAV estimator has small local sensitivity with respect to line impedances in comparison to SHGM, WLS, and LMS estimators. The opposite is the case for measurement sensitivities, where the results show that the LAV estimator has the worst performance among the implemented ones. It can be concluded that the LAV estimator is suitable for networks where line lengths are uncertain, but we have good information about measurement noise characteristics.

In terms of local sensitivities the results show very similar behaviour for the SHGM, WLS, and LMS estimators. However, among the three only the SHGM and the LMS estimators are considered robust in terms of gross measurement errors. Further it needs to be pointed out that the LMS estimator requires the level of redundancy of measurements that is normally not achievable in the distribution networks. Thus, the SHGM estimator based on projection statistics is suggested in cases where line impedances are known with precision, but we are unsure about measurement noise characteristics.

Even though the influence of the line-impedance's uncertainty on the state-vector estimation is smaller for the LAV estimator and for measurement configurations with the prevailing number of PMU measurements (in comparison to those with the prevailing number of power-injection measurements), the line-impedances's uncertainty still influences the calculation of the derived variables (e.g., power flows). Thus, accurate knowledge of line-impedances is crucial for an accurate estimation of the state vector and its derived variables.

The presented approach proved to be useful in the stage of designing the measurement configuration for a state estimation in a real-world network as part of the FP7 SUNSEED project [23].

ACKNOWLEDGMENT

Work was supported by the FP7 SUNSEED project, contract number 619437, http://sunseed-fp7.eu. The authors also acknowledge the financial support from the Slovenian Research Agency (research core funding No. P2-0095).

REFERENCES

[1] D. Della Giustina, M. Pau, P. A. Pegoraro, F. Ponci, and S. Sulis, "Electrical distribution system state estimation: Measurement issues and challenges," *IEEE Instrumentation and Measurement Magazine*, vol. 1094, no. 6969/14, 2014.

[2] T. A. Stuart and C. J. Herczet, "A sensitivity analysis of weighted least squares state estimation for power systems," *IEEE Transactions on Power Apparatus and Systems*, no. 5, pp. 1696–1701, 1973.

[3] D. Macii, G. Barchi, and D. Petri, "Uncertainty sensitivity analysis of wls-based grid state estimators," in *IEEE International Workshop on Applied Measurements for Power Systems (AMPS) Proceedings, 2014*. IEEE, 2014, pp. 1–6.

[4] A. Al-Othman and M. Irving, "Uncertainty modelling in power system state estimation," *IEE Proceedings - Generation, Transmission and Distribution*, vol. 152, no. 2, p. 233, 2005.

[5] ——, "Analysis of confidence bounds in power system state estimation with uncertainty in both measurements and parameters," *Electric Power Systems Research*, vol. 76, no. 12, pp. 1011–1018, Aug. 2006.

[6] C. Rakpenthai, S. Uatrongjit, and S. Premrudeepreechacharn, "State estimation of power system considering network parameter uncertainty based on parametric interval linear systems," *IEEE Transactions on Power Systems*, vol. 27, no. 1, pp. 305–313, Feb. 2012.

[7] S. Chakrabarti and E. Kyriakides, "Pmu measurement uncertainty considerations in wls state estimation," *IEEE Transactions on Power Systems*, vol. 24, no. 2, pp. 1062–1071, May 2009.

[8] S. Chakrabarti, E. Kyriakides, and M. Albu, "Uncertainty in power system state variables obtained through synchronized measurements," *IEEE Transactions on Instrumentation and Measurement*, vol. 58, no. 8, pp. 2452–2458, Aug. 2009.

[9] C. Muscas, S. Sulis, A. Angioni, F. Ponci, and A. Monti, "Impact of different uncertainty sources on a three-phase state estimator for distribution networks," *IEEE Transactions on Instrumentation and Measurement*, vol. 63, no. 9, pp. 2200–2209, Sep. 2014.

[10] R. Minguez and A. J. Conejo, "State estimation sensitivity analysis," *IEEE Transactions on Power Systems*, vol. 22, no. 3, pp. 1080–1091, Aug. 2007.

[11] E. Castillo, A. J. Conejo, C. Castillo, R. Mínguez, and D. Ortigosa, "Perturbation approach to sensitivity analysis in mathematical programming," *Journal of Optimization Theory and Applications*, vol. 128, no. 1, pp. 49–74, Jan. 2006.

[12] R. A. Jabr and B. C. Pal, "Iteratively re-weighted least absolute value method for state estimation," *IEE Proceedings - Generation, Transmission and Distribution*, vol. 150, no. 4, pp. 385–391, 2003.

[13] L. Mili, M. G. Cheniae, N. S. Vichare, and P. J. Rousseeuw, "Robust state estimation based on projection statistics [of power systems]," *IEEE Transactions on Power Systems*, vol. 11, no. 2, pp. 1118–1127, 1996.

[14] L. Mili and P. J. Phaniraj, V.and Rousseeuw, "Least median of squares estimation in power systems," *IEEE Transactions on Power Systems*, vol. 6, no. 2, pp. 511–523, 1991.

[15] L. Mili, M. G. Cheniae, N. S. Vichare, and P. J. Rousseeuw, "Algorithms for least median of squares state estimation of power systems," in *Proceedings of the 35th Midwest Symposium on Circuits and Systems, 1992*. IEEE, 1992, pp. 1276–1283.

[16] A. Abur and A. Gomez Exposito, *Power system state estimation: theory and implementation*. New York, NY: Marcel Dekker, 2004.

[17] R. Jabr, B. Pal, and R. Singh, "Choice of estimator for distribution system state estimation," *IET Generation, Transmission & Distribution*, vol. 3, no. 7, pp. 666–678, Jul. 2009.

[18] R. Jabr, "Primal-dual interior-point approach to compute the L1 solution of the state estimation problem," *IEE Proceedings - Generation, Transmission and Distribution*, vol. 152, no. 3, p. 313, 2005.

[19] U. Kuhar, J. Jurše, K. Alič, G. Kandus, and A. Švigelj, "A unified three-phase branch model for a distribution-system state estimation," in *PES Innovative Smart Grid Technologies Conference Europe (ISGT-Europe), 2016 IEEE*. IEEE, 2016, pp. 1–6.

[20] W. H. Kersting, *Distribution system modeling and analysis*, ser. The electric power engineering series. Boca Raton: CRC Press, 2002.

[21] E. Caro, A. Conejo, and R. Mnguez, "A sensitivity analysis method to compute the residual covariance matrix," *Electric Power Systems Research*, vol. 81, no. 5, pp. 1071–1078, May 2011.

[22] W. H. Kersting, "Radial distribution test feeders," in *Power Engineering Society Winter Meeting, 2001. IEEE*. IEEE, 2001, pp. 908–912.

[23] J. J. Nielsen, H. Ganem, L. Jorguseski, K. Alic, M. Smolnikar, Z. Zhu, N. K. Pratas, M. Golinski, H. Zhang, U. Kuhar, Z. Fan, and A. Svigelj, "Secure real-time monitoring and management of smart distribution grid using shared cellular networks," *IEEE Wireless Communications*, vol. 24, no. 2, pp. 10–17, Apr. 2017.